



Impact of Freeze-Drying Process on Encapsulation of Curcumin: Physicochemical Properties and Release Kinetic Model

Azafilmi Hakiim, Aji Prasetyaningrum*, Nur Rokhati, Mohammad Djaeni

Department of Chemical Engineering, University of Diponegoro, PO Box 50275 Semarang, Indonesia

ARTICLE INFO

Article history:

Received 17 October 2023

Revised 11 November 2023

Accepted 30 November 2023

Published online 01 January 2024

ABSTRACT

Copyright: © 2023 Hakiim *et al.* This is an open-access article distributed under the terms of the [Creative Commons Attribution License](https://creativecommons.org/licenses/by/4.0/), which permits unrestricted use, distribution, and reproduction in any medium, provided the original author and source are credited.

Curcumin (CUR) is a natural polyphenol in turmeric characterized by several health benefits, with limited stability and low bioavailability. Therefore, this research aimed to enhance the physicochemical and morphological properties of CUR using freeze drying (FD) in the encapsulation process with a combination of Alginate (ALG) and Chitosan (CHS) as wall material. The microparticles were made in the form of hydrogel beads with an ALG/CHS wall material in a ratio of 2:1, mixed with CUR dissolved in ethanol. The mixture obtained was injected into a 0.2 M CaCl₂ solution and left for 30 minutes. Subsequently, the hydrogel beads were dried through FD and conventional methods using an oven. The data obtained from ALG/CHS/CUR encapsulated beads by encapsulation efficiency and release kinetic was evaluated using statistical analysis to assess their significance. The Fourier transform infrared (FTIR) results showed that FD method did not cause the loss of the core group, protecting ALG/CHS mixed wall material. Scanning electron microscopy (SEM) showed that FD method had a fibrillation structure with agglomeration, creating an uneven surface resembling a network matrix associated with relatively high porosity. This increased the swelling percentage to 84.55% and boosted encapsulation efficiency to 89.72%. Evaluation of CUR release kinetic from beads treated with FD and non-FD provided an accuracy of R⁻¹ in the Peppas Sahlin model. These results showed that FD in the formulation ALG/CHS/CUR has the potential to improve the physicochemistry and protect the embedded bioactive material.

Keywords: Encapsulation, curcumin, freeze-drying, release

Introduction

Turmeric (*Curcuma longa*) is a natural polyphenol, which yields curcumin (CUR) through extraction.¹ Current research has shown various health benefits of CUR, including antioxidant activities, anti-inhibition of anti-inflammation, anti-microbial activities, wound healing properties, and anti-cancer activity.² Despite these advantages, CUR faces numerous challenges such as low bioavailability, water insolubility, and poor thermal stability, limiting its use in pharmaceuticals.³ One of the most widely investigated technologies to protect and provide the desired properties to active substances is encapsulation.⁴ This technology entails enclosing an active ingredient protected by particles of another substance (wall material) for the isolated, or controlled release of a specific compound.⁵ Encapsulation methods are used based on the core material, desired particle size, physical state, or susceptibility to high temperatures.⁶ This method can affect the characteristics of the final product and properties of the microparticles.⁷ For example, encapsulation by spray and tray drying, which requires heat, will damage the encapsulated bioactive ingredients.⁸ In the case of extrusion, friction during process can reduce the quality of gel bead products.⁹ Although the layer-by-layer deposition method is also effective, it has several disadvantages such as complexity, extended processing time, and higher costs.¹⁰ Another method is ionotropic gelation, which is based on the ability of some polymers to crosslink in the presence of polyvalent Ca²⁺ ions.

*Corresponding author. E mail: aji.prasetyaningrum@che.undip.ac.id
Tel: +628122856097

Citation: Hakiim A, Prasetyaningrum A, Rokhati N, Djaeni M. Impact of Freeze-Drying Process on Encapsulation of Curcumin: Physicochemical Properties and Release Kinetic Model. Trop J Nat Prod Res. 2023; 7(12):5566-5572. <http://www.doi.org/10.26538/tjnpr/v7i12.28>

Official Journal of Natural Product Research Group, Faculty of Pharmacy, University of Benin, Benin City, Nigeria.

Microcapsules made by ion channel gelation have high porosity, enabling rapid diffusion of water and other liquids into and out of the structure.¹¹

However, the main disadvantage of ionotropic gel polymers is low mechanical stability, as the hydrogen surface layer does not completely dry when left at room temperature. To address this issue, development can be achieved by combining ionic gelation methods and complex physical methods with freeze-drying (FD).

FD method is commonly used to dry heat-sensitive bioactive components in producing high-quality dried products at low temperatures and under a vacuum. This method is also used to encapsulate delicate biomaterials on amorphous carbohydrate microstructure matrices.¹² Compared to other alternatives such as coacervation, solvent extraction, and supercritical liquid precipitation, FD method is the most effective and straightforward encapsulation method, significantly improving the response speed of large hydrogels by forming many macrospores.¹³ In encapsulation, coatings or carriers play a significant role, influencing the efficiency percentage, as well as physical and chemical properties that impact the stability of freeze-dried powder.^{6,14}

A coating or encapsulation material surrounds the protected core material during microencapsulation. These encapsulation agents can be selected from various types, including natural and non-natural ingredients, such as Alginate (ALG), Chitosan (CHS), carrageenan, maltodextrin, gum arabic, modified starch, protein, and dextrin.^{6,14,15} Among these agents, maltodextrin is commonly used for microencapsulation of polyphenols due to its low bulk density and viscosity, rapid film formation, the creation of barrier from oxygen, and optimal gel-forming properties.^{5,6,16} However, maltodextrin has a high glycaemic index, which may render microencapsulated products unsuitable for those with diabetes or on a low-carbohydrate diet. Gum arabic is also commonly used as polyphenol polish capable of being used alone or mixed with other encapsulating agents due to its high solubility, high surface activity, low viscosity, high emulsifying

capacity, non-toxic and tasteless.¹⁴ According to Ezhilarasi *et al.*,²⁰ the use of gum Arabic with FD method resulted in high water content. This significant increase was attributed to the higher concentration of protein, which induced aggregation during the freezing process, thereby reducing the availability of interstitial water (the fluid surrounding the cells including the fluid contained between cavities).

A natural polymer called ALG is frequently used in the pharmaceutical industry. This polymer is derived from brown algae and is an anionic linear hydrophilic biopolymer made up of alternating blocks of D-mannuronic acid and L-guluronic acid residues. ALG can be ionically crosslinked by divalent cations to produce a hydrogel.²² However, ALG-based floating carriers have significant limitations, including their high porosity, poor encapsulation efficiency, complex initial release management, and instability in acidic environments. This necessitates the addition of a thickening agent to an ALG hydrogel matrix to modify viscosity and overcome the associated limitations.^{21,23}

CHS is the best option for enhancing ALG performance as a stable gastro-retentive carrier due to its encapsulation efficiency, and ability to provide a modulated drug release profile.²⁴ Furthermore, CHS is a cationic polysaccharide consisting of N-acetyl- β -D-glucosamine and β -D-glucosamine, with a positive charge below neutral pH. This positive charge allows ionic interaction with negatively charged ALG (1-4 linked β -D mannuronate (M) and α -L-guluronate (G) residues), forming a polyelectrolyte complex gel. The complex gel is formed by reacting two oppositely charged CHS with ALG as an alternative to improve the integrity of ALG gel and increase encapsulation efficiency, specific delivery, and controlled release of drugs.^{11,24,25}

However, the use of ALG/CHS as a wall material in microencapsulation with conventional drying still causes high water content and low solubility. To address this issue, this research aimed to develop a complex formulation that combines ALG/CHS using FD method to enhance the solubility, stability, and bioavailability of the encapsulated material.

This research aimed to investigate physicochemical characterization of CUR microencapsulation with ionotropic gelation in an ALG/CHS matrix in FD treatment. These polysaccharides were ionically cross-related with CaCl₂. Furthermore, an investigation was conducted on the consequences of FD on encapsulation efficiency, swelling degree, solubility, and release. The particles obtained were morphologically characterized by SEM and functional groups through FTIR spectroscopy. CUR encapsulation mechanism and kinetic model of the control of release compounds were developed in three mathematical model, namely Kosmeyer Peppas, Peppas Sahlin, and Higuchi equations.

Materials and Methods

Materials

CUR was purchased in January 2023 through pharmpreneurstore in Indonesia, with specifications from Sigma Aldrich, which has serial number-C1386-106USA (purity 95%). Some of the materials purchased from the same shop included sodium ALG with specifications from Sigma Aldrich molar mass 216.12 gm/mol with CAS number 9005-38-3 USA and CHS with MW 190,0000-300,000 g/mol. Furthermore, other materials such as CaCl₂, HCl, and buffer solutions pH 1.2 and pH 6.8 were obtained according to specifications from Merck Chemical Co, Darmstadt, Hesse, Germany, which were stored at air-conditioned room temperature.

Preparation of CUR Encapsulation

Sodium ALG powder of 2% (w/v) was dissolved in water 100 ml and homogenized with a magnetic stirrer for 30 minutes at 28°C. A 1% (w/v) CHS solution was prepared by dissolving it in a buffer of acetic acid/sodium acetate 100 ml (pH 4.7). Subsequently, ALG/CHS solutions were mixed in a 1:1 volume ratio for 30 minutes at 28°C.⁸ To prepare CUR solution, 50 mg of CUR was dissolved in 5 ml ethanol. The solution obtained in the first step was added to ALG/CHS and mixed for 15 minutes using a magnetic stirrer to obtain a homogeneous solution. The beads were made by dripping a mixture of ALG/CHS/CUR solution into a 0.2 M CaCl₂ solution using a syringe and left for 30 minutes to obtain stable beads

constituent. Subsequently, the beads were separated from the CaCl₂ solution, and dried in an oven (non-FD) at 40°C for 24 hours and FD at -70°C, 125 mtorr pressure, for 8 hours.

Characterization of the Particles

Scanning Electron Microscope (SEM) Analysis

Encapsulation of CUR in ALG/CHS results was analyzed using surface morphology with machine SEM (JSM-6510LV JEOL, Japan) magnification is 7500x.

Fourier Transform Infrared Spectroscopy (FTIR) Analysis

FTIR testing of CUR encapsulation in an ALG/CHS matrix was carried out using the Perkin Elmer Spectrum IR 10.6.1 spectrophotometer (Perkin Elmer Inc., USA) equipped with functional groups in the wavelength range of 4000 - 450 cm⁻¹. Subsequently, the data obtained was compared and analyzed to identify changes that occurred in the chemical structure resulting from FD and non-FD samples.

Percentage Encapsulation Efficiency

Encapsulation efficiency was performed through an indirect method by determining the amount of bioactive agent that was not incorporated into the beads after ALG/CHS beads were dropped into a CaCl₂ solution. Specifically, 2 ml of CaCl₂ solution was taken and added with 2 ml of AlCl₃ and 2 ml of KCH₃COO. This was followed by the determination of bioactive content using a Genesis 20 UV-Vis spectrophotometer at 423 nm. The calculation of encapsulation efficiency:²⁸

$$EE (\%) = \frac{Q_t - Q_r}{Q_t} \times 100 \quad (1)$$

Q_t is the amount of bioactive in CUR and Q_r is the bioactive CUR present in CaCl₂ solution after encapsulation.

Swelling Analysis

Swelling analysis of dry CUR encapsulated beads was performed based on pH 6.8 of the solution. Beads of 0.2 g were soaked in 10 ml phosphate buffer (pH=6.8). The swelling of CUR encapsulation was calculated using the following formula for each.⁸

$$\text{Swelling} = \left(\frac{m_{\text{wet}}}{m_{\text{dry}}} \right) \cdot 100 \quad (2)$$

CUR Release Test

The system for releasing bioactive CUR in capsules was tested at different pH values of 1.2 and 6.8. A sample of 0.2 g of CUR encapsulated in the best formulation was into 30 ml of pH 1.2 and 6.8 solution and soaked for 24 hours. At the specified time interval, 5 ml samples were taken for analysis using a spectrophotometer at a wavelength of 423 nm to determine release of bioactive CUR at each time point. Subsequently, the determination of release mechanism of CUR encapsulated in the form of beads was plotted in three mathematical model. The experimental data is needed in all model calculations from the equilibrium time (M_{eq}) and the amount of bioactive substances released at time t (M_t). These data were incorporated into the empirical formula below:²⁷

Korsmeyer-Peppas model

$$\frac{M_t}{M_{eq}} = k_1 t^n \quad (3)$$

where k₁ is the rate depending on the structural and geometrical properties of the discharge system, and n is called the diffusion index which determines release mechanism. For delivery system with n ≤ 0.43, release mechanism is the Fickian mechanism, showing a normal diffusion of encapsulated molecules through a chemical potential gradient. At n values ≥ 0.85, release mechanism includes case II gradual release. Case II stages include mechanisms related to stress and state transitions in the self-assembly of the swollen polymer in water or biological fluids. Meanwhile, 0.43 < n < 0.85, release is a non-fictional release with diffusion and relaxation contributing to release.

Peppas-Sahlin model

$$\frac{M_t}{M_{eq}} = k_1 t^m + k_2 t^{2m} \quad (4)$$

This release kinetic model applies diffusion and relaxation mechanisms in the drug release process. To determine the biological activity release, the F value represents the Fickian diffusion contribution and the R value represents the relaxation contribution. The R/F ratio shows the contribution of Fickian relaxation and diffusion in drug release. At R/F = 1, release mechanism also contributes to erosion (relaxation) and diffusion. For R/F > 1, recovery (erosion) dominates, and for R/F < 1, expansion (erosion) or diffusion prevails. The relaxation ratio (R) can be calculated with the Fickian contribution (F):

$$\frac{R}{F} = \frac{k_2}{k_1} t^m \quad (5)$$

k_2 is the relaxation kinetic constant from the Peppas-Sahlin equation, k_1 is the Fickian diffusion rate constant.

Higuchi model

$$\frac{M_t}{M_{eq}} = k_h t^{0.5} \quad (6)$$

k_h is the Higuchi coefficient. High values of the correlation coefficient of the fit can be interpreted as the dominant mechanism of bioactive release as a diffuse release mechanism.

Results and Discussion*Characterization of CUR Encapsulation Beads by FTIR*

FTIR analysis was carried out to confirm the existence or interaction of the samples obtained, as shown in Figure 1, with corresponding adjustments for the coverage areas presented in Table 1. Furthermore, the FTIR spectra of the microcapsule granules in FD treatment were compared to conventional (non-FD). In FD spectrum, a more complex peak was observed for the formation of molecular bond interactions between ALG/CHS and CUR, with data strengthening at the peak of 3337 cm^{-1} , showing phenolic hydroxyl vibrations. A significant difference was also observed in the intensity of the absorbance peak in encapsulation results of FD and non-FD methods, as shown in Figure 1.

A significant peak was observed in CUR spectrum of 3291 cm^{-1} , as shown in Figure 1. This value was close to the peak of the phenolic-OH bond interaction reported by Silva *et al.*³² at 3438 cm^{-1} , as well as Chiaooprakobkij *et al.*³³ and Hashim *et al.*³⁴ at 3509 cm^{-1} . According to Munajad *et al.*, the peak absorption intensity correlated with temperature.

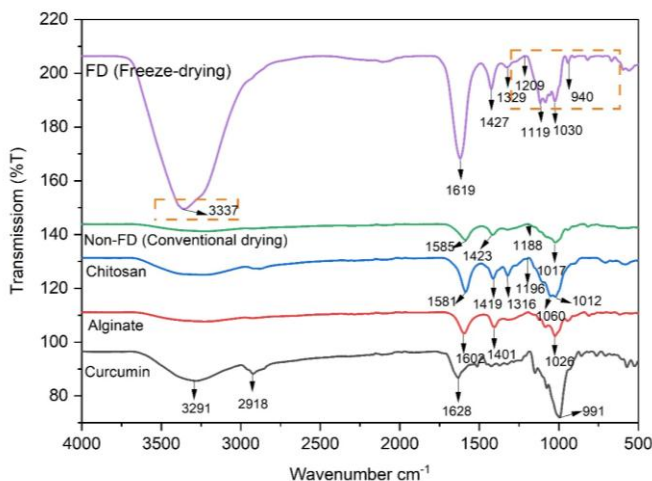


Figure 1. FTIR spectra for CUR encapsulation

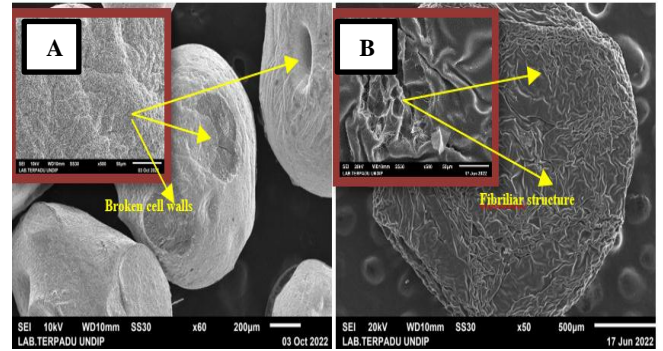


Figure 2: SEM images of encapsulation CUR beads: A) ALG/CHS/CUR Non-FD; B) ALG/CHS/CUR with FD

The intensity for FD peak for freeze-dried sample showed a higher number compared to non-FD, which was broad and did not show the peak appearance associated with the deformation of the OH groups.³⁵ These results were consistent with Liew *et al.*³⁶, where the content of phenolic compounds was significantly high in freeze-dried powder compared to oven drying in *Clitoria ternatea* (flowers) encapsulation. This variation occurred due to the breaking of hydrogen bonds, causing a decrease in molecular weight.

The sharp peak of FD microbeads at the total intensity spectrum of 1427 cm^{-1} and 1619 cm^{-1} showed a higher level of interaction between the Na-group and the secondary amine absorption group (>N-H bend) compared to non-FD microbeads, which had peaks at 1585 cm^{-1} and 1423 cm^{-1} , respectively. However, both values were close to the results of sample ALG in spectrum Na-grup 1602 cm^{-1} and CHS spectrum N-H bend in 1423 cm^{-1} , as shown in Figure 1. Bayu *et al.*³³ also reported the association of the Na-group in ALG 1420 cm^{-1} and the N-H bend 1620 cm^{-1} . FD process did not cause loss of the core group (bioactive), which was protected using a mixture of ALG/CHS as wall material.

Morphological Properties of CUR Encapsulation Beads

SEM images were taken to determine the morphologies that provided a topographical description of the sample through direct visualization and surface features at a microscopic level of our system.

Figure 2A shows the structure on the surface of the encapsulated beads using non-FD. These beads have a rough surface wall structure due to direct heat penetration through encapsulation material. Conventional drying uses setting conditions in the oven, where the evaporation mechanism usually occurs at high temperatures. Consequently, the dry part of the beads passes through chemical changes (gelatinization, caramelization, and denaturation), which causes a crust to form on the surface, providing an obstacle to the diffusion of water vapor from the wet part to the surrounding air. This process results in an excessively dry final product on the outside while retaining moisture in the middle. Non-FD mechanisms have the potential to change the surface structure of the cell walls and spaces between tissue cell, resulting in damaged cell walls. This damage reduces contact between cells and breaks down the cell structure.³⁸ Meanwhile, FD method occurs through a sublimation mechanism at cold temperatures (-70°C), preventing process such as gelatinization, caramelization, and denaturation. This phenomenon causes no change or crust formation on the dry part of the encapsulated beads, facilitating efficient diffusion of water vapor from the wet part into the ambient air. This shows that the beads formed in FD process with ALG/CHS/Cur formula have strong mechanical properties, ensuring the presentation of the bioactive parts. The resulting FD product shows maximum drying.

FD structure in encapsulation showed a smoother, dense, and porous surface compared to non-FD surface, as presented in Figure 2B. According to Hau *et al.*³⁹, the physicochemical properties of hydrolyzed protein powder from the yellow stripe by FD showed that the frozen powder product had a fiber stripe with a 'collapsed-building' shape. Similarly, Silva *et al.*³² observed that the structure of freeze-dried hydrogel beads appeared to be foam pores. FD

encapsulation process also showed that the fibrillation structure showed by agglomeration in the form of an uneven surface was a tissue matrix associated with relatively high water solubility and weak mechanical properties. This showed that the hydroxyl groups present in the walls of ALG and CHS materials by FD reduced hydrophobic interactions and increased hydrogen bonds with water, thereby facilitating dissolution.³⁶

The morphology observed can also be related to the large particle size produced, where FD treatment showed a larger particle size of 109.207 μm compared to 70.781 μm obtained in non-FD. The performance of drug release was highly influenced by particle size. Consequently, when particle size is excessively small, the drug carrier matrix enters the cell and precipitates inside, potentially disrupting the cell cycle. When particle size is large, the rate of drug degradation becomes very sluggish, leading to decreased efficiency as encapsulation particle size increases.³⁷ In this research, it was discovered that encapsulation

efficiency of FD method was greater compared to non-FD with values of 89.72% and 54.65% respectively.

The morphological results of the dry matrix beads from FD and non-FD methods correlated with the swelling test. This was confirmed by soaking the dry beads from both methods using a buffer solution of pH 6.8. The swelling test is significant in drug delivery, incorporating the absorption of liquid into the matrix, which interferes with release kinetic.³⁷ The results presented in Figures 3A and 3B are expected to pass through a swelling process after contact with the pH 6.8 buffer. This phenomenon occurred due to the hydration of hydrophilic groups such as hydroxyl, amine, carboxyl, and alcohol groups. The swelling rate of FD microbeads at 84.55% was higher than non-FD, as shown in Figure 3D, due to the morphological appearance forming a porous network matrix. Consequently, the liquid penetrates the beads and fills the pores between the polymer chains, causing swelling that occurs with or without bead degradation.

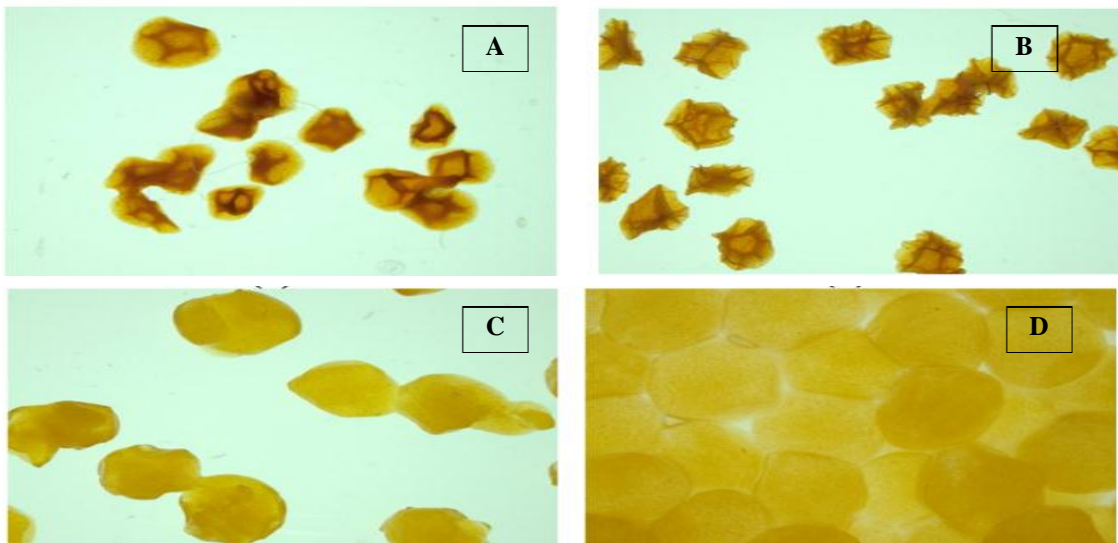


Figure 3: Optical image magnification 2x of CUR encapsulation beads: (A) before swelling non-FD B) before swelling FD and (C) after swelling non-FD, (D) after swelling FD

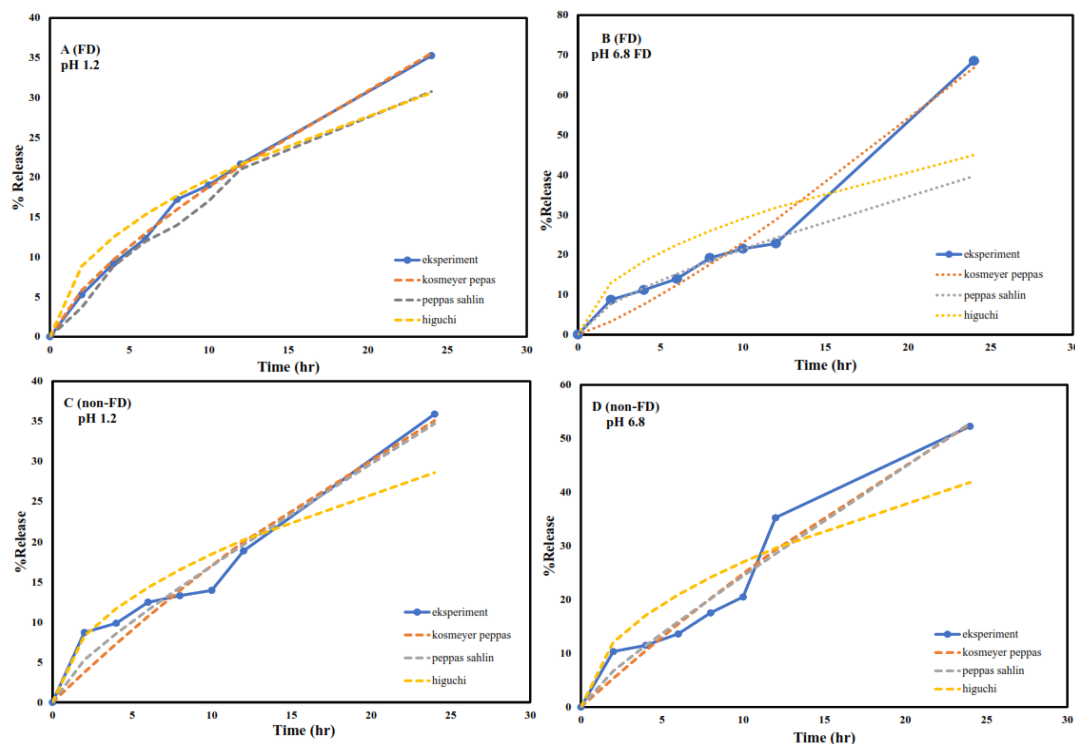


Figure 4: Release kinetic CUR encapsulation plots:(A) FD pH 1.2; (B) FD pH 6.8; (C) non-FD pH 1.2; (D) non-FD pH 6.8

Table 1: FTIR spectra

Wavenumber Range (cm ⁻¹)	Functional Groups	Reference
3200-3500	Phenolic O-H	28
3570-3200	O-H Stretching	32
2935-2915	C-H Stretch	33
1680-1620	C=C Stretch	33
1650-1550	Secondary amine (>N-H bend)	33
1614-1424	Na-groups	25
1400-1403	Symmetric stretching vibration of COO-	33
1300-700	C-C Vibration	33
1100-1010	C-O	33

Table 2: Kinetic release CUR encapsulation

System	Higuchi		Kosmeyer Peppas model			Peppas Sahlin model				
	k _h	R ²	k ₁	n	R ²	k ₁	k ₂	m	R/F	R ²
pH 1.2										
FD	6.25	0.91	3.51	0.72	0.99	1.78	2.19	0.41	1.17	0.99
non-FD	8.54	0.93	3.34	2.06	0.97	1.74	2.06	0.48	1.18	0.97
pH 6.8										
FD	9.17	0.91	1.40	1.20	0.98	4.08	1.00	0.47	0.24	0.95
non-FD	5.84	92.8	2.81	0.78	0.97	2.90	0.42	0.57	0.14	0.98

Release Kinetic of CUR Encapsulation

The experimental data were plotted in different kinetic model to analyze release mechanism shown in Figure 4 and Table 2. The absorption of water molecules followed by drug desorption described the underlying principles of encapsulation release kinetic. The rate of drug release is controlled by the dry polymer (glass) hydrogel resistance to changing shape and volume during the hydration process. This resistance is controlled by the composition of hydrogel and the density of its crosslinks.³⁸

The cumulative release rate of CUR from ALG/CHS/CUR is shown graphically in Figure 4 for 24 hours in simulated stomach (pH 1.2) and intestinal (pH 6.8) fluids. Release rate of % ALG/CHS/CUR was lower at pH 1.2 compared to pH 6.8 due to ALG solubility and the creation of carboxyl ion groups. In acidic environments, ALG dissociates and becomes insoluble, showing its ability to protect CUR levels in the gastric environment.³⁹ Kinetic parameter characteristics shown by the hydrogel beads in ALG/CHS/CUR with FD and non-FD methods were obtained after data acquisition with the three mathematical model equations used, namely Peppas Kosmeyer, Peppas Sahlin, and Higuchi. Based on Table 2, release of CUR from all hydrogel granules corresponded to all model used with the best statistical model of Kosmeyer Peppas, followed by Peppas-Sahlin, and Higuchi. A statistical show was evident from the correlation coefficients (R²~1.0) obtained for the Kosmeyer Peppas and Peppas-Sahlin kinetic model. Meanwhile, the Higuchi model showed that release mechanism is primarily diffusion.

The Higuchi model does not appear to fit the data observed compared to the Peppas-Kosmeyer and Peppas-Sahlin model. This suggests that the relaxation factor is wholly excluded from the mechanism following CUR release from the beads, showing no relaxation at both pH 1.2 and pH 6.8, as shown in Table 1. Similar results are obtained with the best fitting from the Kosmeyer-Peppas model, where the down-value at pH 1.2 is 0.43 < 0.43. For n < 0.85, release mechanism is dominated by diffusion followed by relaxation. Meanwhile, at pH 6.8, n ≥ 0.85 is a relaxation mechanism for bioactive release, facilitated by stress and transitions.

From the experimental results, pH 1.2 showed that the value k₁ on FD (k₁= 3.51) hydrogel beads was greater compared to non-FD (k₁=2.81). This showed that release rate of bioactive assisted by FD was greater

than non-FD. At pH 6.8, the constant rate of release of bioactive non-FD (k₁=2.81) was greater than that of FD (k₁=1.40). This showed that the mechanism of bioactive transport consisting of stress and transition in release of bioactive in FD was more controlled than the non-FD method.

In the Peppas Sahlin model, the ratio of relaxation (R) to the Fickian contribution (F) is presented in Table 2, which is calculated by the R/F factor (equation 2). When R/F = 1, it creates contributes to erosion (relaxation) and diffusion. For R/F > 1, relaxation (erosion) predominates, while R/F < 1 shows diffusion predominates. The R/F value of the beads under FD and non-FD conditions at pH 1.2 had an R/F ratio > 1, while pH 6.8 showed an R/F ratio < 1. At pH 1.2 conditions, the R/F value at non-FD was slightly larger than FD, showing that NF conditions predominate for faster erosion (relaxation) than FD. Meanwhile, the condition of pH 6.8 showed that the R/F value of FD was greater than non-FD, showing higher control of diffusion dominance.

The observation is related to the SEM study in Figure 2, which shows the formation of different pores on the dry bead surface in FD and non-FD methods. This refers to the level of drug solubility and the swelling mechanism that occurs during matrix release. Furthermore, dry beads in FD method showed an uneven and porous wall surface, increasing the length of the diffusion path which allows the solvent to penetrate the matrix and form a viscous gel. The non-FD method shows damage to the smooth surface of the wall, restricting the solvent capability to penetrate the matrix and prevent swelling.

Conclusion

The FD method showed promising potential to improve CUR encapsulation in ALG/CHS matrices for the protection of bioactive components. Based on the results, CUR encapsulation efficiency by FD method reached 89.72%, and the swelling rate was found to be 84.55%. Analysis of release kinetic of the resulting beads with FD and NF using the Higuchi, Kosmeyer Peppas, and Peppas Sahlin equation model showed a tendency for the dominance properties that occurred in the beads produced. Moreover, further research regarding optimizing the performance of ALG/CHS wall materials by adding emulsifiers in FD could provide further benefits.

Conflict of Interest

The authors declare no conflict of interest.

Authors' Declaration

The authors hereby declare that the work presented in this article is original and that any liability for claims relating to the content of this article will be borne by them.

Acknowledgments

The authors are grateful to Diponegoro University for facilitating this research and providing financial state the grant number through the Riset Publikasi Internasional Bereputasi Tinggi (RPIBT) research grant. The authors are also grateful to the Faculty of Chemical Engineering, Diponegoro University, Chemical Engineering Laboratory for the convenience in carrying out this research.

References

- Wang H, Gong X, Guo X, Liu C, Fan YY, Zhang J, Niu B, Li W. Characterization, Release, and Antioxidant Activity of Curcumin-Loaded Sodium Alginate/ZnO Hydrogel Beads. *Int J Biol Macromol*. 2019; 121: 1118-1125. <https://doi.org/10.1016/j.ijbiomac.2018.10.121>.
- Liu YM, Zhang QZ, Xu DH, Fu YW, Lin DJ, Zhou SY, Li JP. Antiparasitic Efficacy of Curcumin from *Curcuma longa* Against *Ichthyophthirius multifiliis* in Grass Carp. *Vet Parasitol*. 2017; 236: 128-136. <https://doi.org/10.1016/j.vetpar.2017.02.011>.
- Pantwalawalkar J, More H, Bhange D, Patil U, Jadhav N. Novel Curcumin Ascorbic Acid Cocrystal for Improved Solubility. *J Drug Deliv Sci and Technol*. 2021; 61: 102233. <https://doi.org/10.1016/j.jddst.2020.102233>.
- Sarheed O, Dibi M, Ramesh KVRNS. Studies on The Effect of Oil and Surfactant on The Formation of Alginate-Based O/W Lidocaine Nanocarriers Using Nanoemulsion Template. *Pharmaceutics*. 2020; 12(12): 1-21. <https://doi.org/10.3390/pharmaceutics12121223>.
- Papoutsis K, Golding JB, Vuong Q, Pristijono P, Stathopoulos CE, Scarlett CJ, Bowyer M. Encapsulation of Citrus by-Product Extracts by Spray-Drying and Freeze-Drying Using Combinations of Maltodextrin With Soybean Protein and κ -carrageenan. *Foods*. 2018;7(7):1-12. <https://doi.org/10.3390/foods7070115>.
- Wilkowska A, Ambroziak W, Czynowska A, Adamiec J. Effect of Microencapsulation by Spray-Drying and Freeze-Drying Technique on the Antioxidant Properties of Blueberry (*Vaccinium myrtillus*) Juice Polyphenolic Compounds. *Polish J Food Nutr Sci*. 2016; 66(1):11-16. <https://doi.org/10.1515/pjfn-2015-0015>.
- Kandimalla R, Kalita S, Choudhury B, Dash S, Kalita K, Kotoky J. Chemical Composition and Anti-Candidiasis Mediated Wound Healing Property of *Cymbopogon nardus* Essential Oil on Chronic Diabetic Wounds. *Front Pharmacol*. 2016;7(JUN):1-8. <https://doi.org/10.3389/fphar.2016.00198>.
- Iurciuc-Tincu CE, Atanase LI, Ochiuz L, Jérôme C, Sol V, Martin P, Popa M. Curcumin-Loaded Polysaccharides-Based Complex Particles Obtained by Polyelectrolyte Complexation and Ionic Gelation. I-Particles Obtaining and Characterization. *Int J Biol Macromol*. 2020; 147: 629-642. <https://doi.org/10.1016/j.ijbiomac.2019.12.247>.
- Tsirigotis-Maniecka M, Gancarz R, Wilk KA. Preparation and Characterization of Sodium Alginate/Chitosan Microparticles Containing Esculin. *Colloids Surfaces A Physicochem Eng Asp*. 2016; 510: 22-32. <https://doi.org/10.1016/j.colsurfa.2016.08.029>.
- Pereira A da S, Diniz MM, De Jong G, Filho HSG, dos Anjos MJ, Finotelli PV, Fontes-Sant'Ana GC, Amaral PFF. Chitosan-Alginate Beads as Encapsulating Agents for *Yarrowia lipolytica* lipase: Morphological, Physico-Chemical and Kinetic Characteristics. *Int J Biol Macromol*. 2019; 139: 621-630. <https://doi.org/10.1016/j.ijbiomac.2019.08.009>.
- Rezvankhah A, Emam-Djomeh Z, Askari G. Encapsulation and Delivery of Bioactive Compounds Using Spray and Freeze-Drying Techniques: A Review. *Trends Food Sci Technol*. 2020; 3: 235-258. <https://doi.org/10.1080/07373937.2019.1653906>.
- Pudziuelyte L, Marksa M, Sosnowska K, Winnicka K, Morkuniene R, Bernatoniene J. Freeze-Drying Technique for Microencapsulation of *Elsholtzia ciliata* Ethanolic Extract Using Different Coating Materials. *Molecules*. 2020; 25(9): 1-16. <https://doi.org/10.3390/molecules25092237>.
- Šturm L, Osojnik Črnič IG, Istenič K, Ota A, Megušar P, Slukan A, Humar M, Levic S, Nedović V, Kopinč R, Deželak M, Gonzales AP, Ulrih NP. Encapsulation of Non-Dewaxed Propolis by Freeze-Drying and Spray-Drying Using Gum Arabic, Maltodextrin and Inulin as Coating Materials. *Food and Bioprod Process*. 2019; 116: 196-211. <https://doi.org/10.1016/j.fbp.2019.05.008>.
- Kuck LS, Noreña CPZ. Microencapsulation of Grape (*Vitis labrusca* var. *Bordo*) Skin Phenolic Extract Using Gum Arabic, Polydextrose, and Partially Hydrolyzed Guar Gum as Encapsulating Agents. *Food Chem*. 2016; 194: 569-576. <https://doi.org/10.1016/j.foodchem.2015.08.066>.
- Rezvankhah A, Emam-Djomeh Z, Askari G. Encapsulation and Delivery of Bioactive Compounds Using Spray and Freeze-drying Techniques: A Review. *Dry Technol*. 2020; 38(1-2): 235-258. <https://doi.org/10.1080/07373937.2019.1653906>.
- Jeyakumari A. Microencapsulation of Bioactive Food Ingredients and Controlled Release - A Review. *MOJ Food Process Technol*. 2016;2(6). <https://doi.org/10.15406/mojfpt.2016.02.00059>.
- Cano-Higuaita DM, Vélez HAV, Telis VRN. Microencapsulation of Turmeric Oleoresin in Binary and Ternary Blends of Gum Arabic, Maltodextrin and Modified Starch. *Ciencia Agrotecnologia*. 2015; 39(2): 173-182. <https://doi.org/10.1590/S1413-70542015000200009>.
- Chranioti C, Tzia C. Arabic Gum Mixtures as Encapsulating Agents of Freeze-Dried Fennel Oleoresin Products. *Food Bioprocess Technol*. 2014;7(4):1057-1065. <https://doi.org/10.1007/s11947-013-1074-z>.
- Ezhilarasi PN, Indrani D, Jena BS, Anandharamkrishnan C. Freeze Drying Technique for Microencapsulation of Garcinia Fruit Extract and Its Effect on Bread Quality. *J Food Eng*. 2013; 117(4): 513-520. <https://doi.org/10.1016/j.jfoodeng.2013.01.009>.
- Sayeesh P, Joy R, Pradeep N, John F, George J. Alginate/ κ -Carrageenan and Alginate/Gelatin Composite Hydrogel Beads for Controlled Drug Release of Curcumin. *Adv Mater Lett*. 2019; 10(7): 508-514. <https://doi.org/10.5185/amlett.2019.2149>.
- Postolović KS, Antonijević MD, Ljujić B, Kovačević MM, Janković MG, Stanić ZD. pH-Responsive Hydrogel Beads Based on Alginate, κ -Carrageenan and Poloxamer for Enhanced Curcumin, Natural Bioactive Compound, Encapsulation and Controlled Release Efficiency. *Molecules*. 2022; 27(13). <https://doi.org/10.3390/molecules27134045>.
- Ramdhan T, Ching SH, Prakash S, Bhandari B. Physical and Mechanical Properties of Alginate Based Composite Gels. *Trends Food Sci Technol*. 2020; 106: 150-159. <https://doi.org/10.1016/j.tifs.2020.10.002>.
- Akbari-Alavijeh S, Shaddel R, Jafari SM. Encapsulation of Food Bioactives and Nutraceuticals by Various Chitosan-Based Nanocarriers. *Food Hydrocoll*. 2020; 105. <https://doi.org/10.1016/j.foodhyd.2020.105774>.

24. Shamsuri AA, Siti Nurul SNA. Functional Properties of Biopolymer-Based Films Modified With Surfactants: A Brief Review. *Processes*. 2020; 8(9): 1-14. <https://doi.org/10.3390/pr8091039>.
25. Nalini T, Basha SK, Mohamed Sadiq AM, Kumari VS, Kaviyarasu K. Development and Characterization of Alginate/Chitosan Nanoparticulate System for Hydrophobic Drug Encapsulation. *J Drug Deliv Sci Technol*. 2019; 52: 65-72. <https://doi.org/10.1016/j.jddst.2019.04.002>.
26. Cirri M, Maestrelli F, Scuota S, Bazzucchi V, Mura P. Development and Microbiological Evaluation of Chitosan and Chitosan-Alginate Microspheres for Vaginal Administration of Metronidazole. *Int J Pharm*. 2021; 598: 120375. <https://doi.org/10.1016/j.ijpharm.2021.120375>.
27. Silva JM, Silva E, Reis RL. Therapeutic Deep Eutectic Solvents Assisted The Encapsulation of Curcumin in Alginate-Chitosan Hydrogel Beads. *Sustain Chem Pharm*. 2021; 24: 100553. <https://doi.org/10.1016/j.scp.2021.100553>.
28. Chiaoprakobkij N, Suwanmajo T, Sanchavanakit N, Phisalaphong M. Curcumin-Loaded Bacterial Cellulose/Alginate/Gelatin as A Multifunctional Biopolymer Composite Film. *Molecules*. 2020; 25(17): 1-18. <https://doi.org/10.3390/molecules25173800>.
29. Hashim AF, Hamed SF, Abdel Hamid HA, Abd-Elsalam KA, Golonka I, Musiał W, El-Sherbiny IM. Antioxidant and Antibacterial Activities of Omega-3 Rich Oils/Curcumin Nanoemulsions Loaded in Chitosan and Alginate-Based Microbeads. *Int J Biol Macromol*. 2019; 140: 682-696. <https://doi.org/10.1016/j.ijbiomac.2019.08.085>.
30. Munajad A, Subroto C, Suwarno. Fourier Transform Infrared (FTIR) Spectroscopy Analysis of Transformer Paper in Mineral Oil-Paper Composite Insulation Under Accelerated Thermal Aging. *Energies*. 2018; 11(2). <https://doi.org/10.3390/en11020364>.
31. Liew SY, Mohd Zin Z, Mohd Maidin NM, Mamat H, Zainol MK. Effect of The Different Encapsulation Methods on The Physicochemical and Biological Properties of *Clitoria ternatea* Flowers Microencapsulated In Gelatine. *Food Res*. 2020; 4(4): 1098-1108. [https://doi.org/10.26656/fr.2017.4\(4\).033](https://doi.org/10.26656/fr.2017.4(4).033).
32. Bayu A, Nandiyanto D, Oktiani R, Ragadhita R. How to Read and Interpret FTIR Spectroscopy of Organic Material. *Indonesian J Sci & Technol*. 2019; 4(1): 97-118. <https://doi.org/10.17509/ijost.v4i1.15806>.
33. Li Y, Kong M, Feng C, Liu WF, Ya Liu, Chen XG. Preparation And Property of Layer-by-Layer Alginate Hydrogel Beads Based on Multi-Phase Emulsion Technique. *J Sol-Gel Sci Technol*. 2012;62(2):217-226. <https://doi.org/10.1007/s10971-012-2712-z>.
34. Hau EH, Mohd Zin Z, Zuraidah N, Shaharudin NA, Zainol MK. Physicochemical Properties of Powdered Protein Hydrolysate From Yellowstripe Scad (*Selaroides leptolepis*) Fish. *Int Food Res J*. 2018; 25(6): 2553-2559.
35. Thai H, Thuy Nguyen C, Thi Thach L, Tran MT, Mai HD, Nguyen TTT, Le GD, Can MV, Tran LD, Bach GL, Ramadass K, Sathish CI, Le QV. Characterization of Chitosan/Alginate/Lovastatin Nanoparticles and Investigation of Their Toxic Effects in Vitro and in Vivo. *Sci Rep*. 2020; 10(1): 1-15. <https://doi.org/10.1038/s41598-020-57666-8>.
36. Bastan FE, Erdogan G, Moskalewicz T, Ustel F. Spray Drying of Hydroxyapatite Powders: The Effect of Spray Drying Parameters And Heat Treatment on The Particle Size And Morphology. *J Alloys and Compd*. 2017; 724: 586-596. <https://doi.org/10.1016/j.jallcom.2017.07.116>.
37. Rizwan M, Yahya R, Hassan A, Yar M, Azzahari AD, Selvanathan V, Sonsudin F, Abouloula CN. pH Sensitive Hydrogels in Drug Delivery: Brief History, Properties, Swelling, and Release Mechanism, Material Selection and Applications. *Polymers*. 2017; 9(4). <https://doi.org/10.3390/polym9040137>.
38. Zhang Z, Zhang R, Zou L, Chen L, Ahmed Y, Al Bishri W, Balamash K, McClements DJ. Encapsulation of Curcumin in Polysaccharide-Based Hydrogel Beads: Impact of Bead Type on Lipid Digestion and Curcumin Bioaccessibility. *Food Hydrocoll*. 2016; 58: 160-170. <https://doi.org/10.1016/j.foodhyd.2016.02.036>.
39. Aliabbasi N, Fathi M, Emam-Djomeh Z. Curcumin: A Promising Bioactive Agent for Application in Food Packaging Systems. *J Environ Chem Eng*. 2021; 9(4): 105520. <https://doi.org/10.1016/j.jece.2021.105520>.